Birth of the Biscane

Michael Maier-Gerber,[1] Florian Pantillon,[1] Enrico Di Muzio,[1] Michael Riemer,[2] Andreas H. Fink[1] and Peter Knippertz[1]

[1]*Institute of Meteorology and Climate Research, Karlsruhe Institute of Technology, Germany*

[2]*Institute of Atmospheric Physics, Johannes Gutenberg University, Mainz, Germany*

Weather – August 2017, Vol. 72, No. 8

Introduction

Tropical cyclones form over the high sea surface temperatures (SSTs) of tropical oceans, usually in an environment of low vertical wind shear. When an Atlantic tropical cyclone features sustained winds over 64kn, it is called a hurricane. Occasionally, tropical-like cyclones form at higher latitudes, originating from mid-latitude storms that undergo a process known as tropical transition (Davis and Bosart, 2004), thereby acquiring typical traits of tropical cyclones such as a warm core, axial symmetry and a cloud-free eye. This process can occur over the Mediterranean (Billing *et al.*, 1983; Ernst and Matson, 1983), and the resulting tropical-like storm is referred to as a Medicane (from *Medi*terranean hurri*cane*; e.g. Fita *et al.*, 2007).

Although the Mediterranean SST is not as high as that of the tropical North Atlantic, the thermodynamic disequilibrium between warm, moist lower-level air and cold upper-level air associated with an upper-level cut-off low is a suitable environment for tropical transition (Emanuel, 2005). In addition, the presence of a cut-off can decrease the vertical wind shear and enhance upright convection, thus promoting the formation of a tropical-like storm. Medicanes are smaller and shorter lived than actual hurricanes and only occasionally reach hurricane-force intensity. Nevertheless, they are amongst the most intense storms that occur in the Mediterranean and can cause severe damages in coastal areas, due to strong winds and large amounts of rainfall.

On 15 September 2016, a surface low over the Bay of Biscay – named *Stephanie* by the Free University in Berlin – exhibited a striking cloud-free central area in satellite imagery as it was located about 100km to the north of the Spanish coast (Figure 1). As detailed in the next sections, this storm shared common tropical-like features with Medicanes in its structure and development. By analogy with its Mediterranean counterparts, we propose to name this storm a 'Biscane' (*Bis*cay hurri*cane*). To the best of the authors' knowledge, no such storm has ever been documented in this region.

Synoptic evolution

The main ingredients for the synoptic development of this system were a cut-off detaching from an elongated mid-latitude trough and the surface low itself. During the second week of September, a blocking situation prevailed over Europe and was accompanied by new maximum temperature records for the period. Figure 2(a) shows the synoptic flow pattern on 13 September. A trough upstream of the blocking was elongating meridionally over the eastern North Atlantic and dipped as far south as the Strait of Gibraltar. At this stage, an associated cold front was collocated with the leading edge of the trough and therefore oriented in a north–south direction (Figure 2(d)). Later that day, a cut-off formed over the northern Iberian Peninsula, where it maintained its position for the next 2 days (Figure 2(b) and (c)).

Meanwhile, a surface low formed over the Bay of Biscay off the Spanish coast and rotated cyclonically around the quasi-stationary cut-off. Initially, the low moved northward, parallel to the western coast of France (Figure 2(e)), until it turned to the west. Located to the southwest of Brittany, the low distorted the cold front and eventually underwent a classical occlusion process on 14 September (Figure 2(f)). The cut-off and the surface low became increasingly aligned in the vertical, resulting in a more barotropic structure. Both the cut-off and the surface low then moved southeastward towards the Spain–France border, where the surface low made landfall and decayed rapidly on 16 September (not shown).

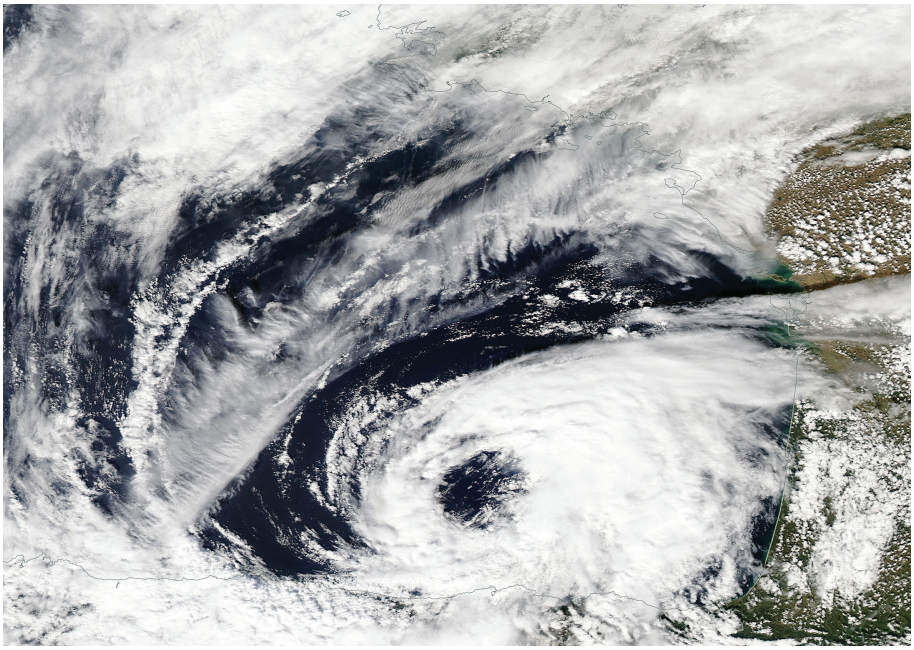

Figure 1. MODIS satellite observation of storm Stephanie over the Bay of Biscay on 15 September 2016 at 1318 UTC. The cloud-free central area is clearly visible.

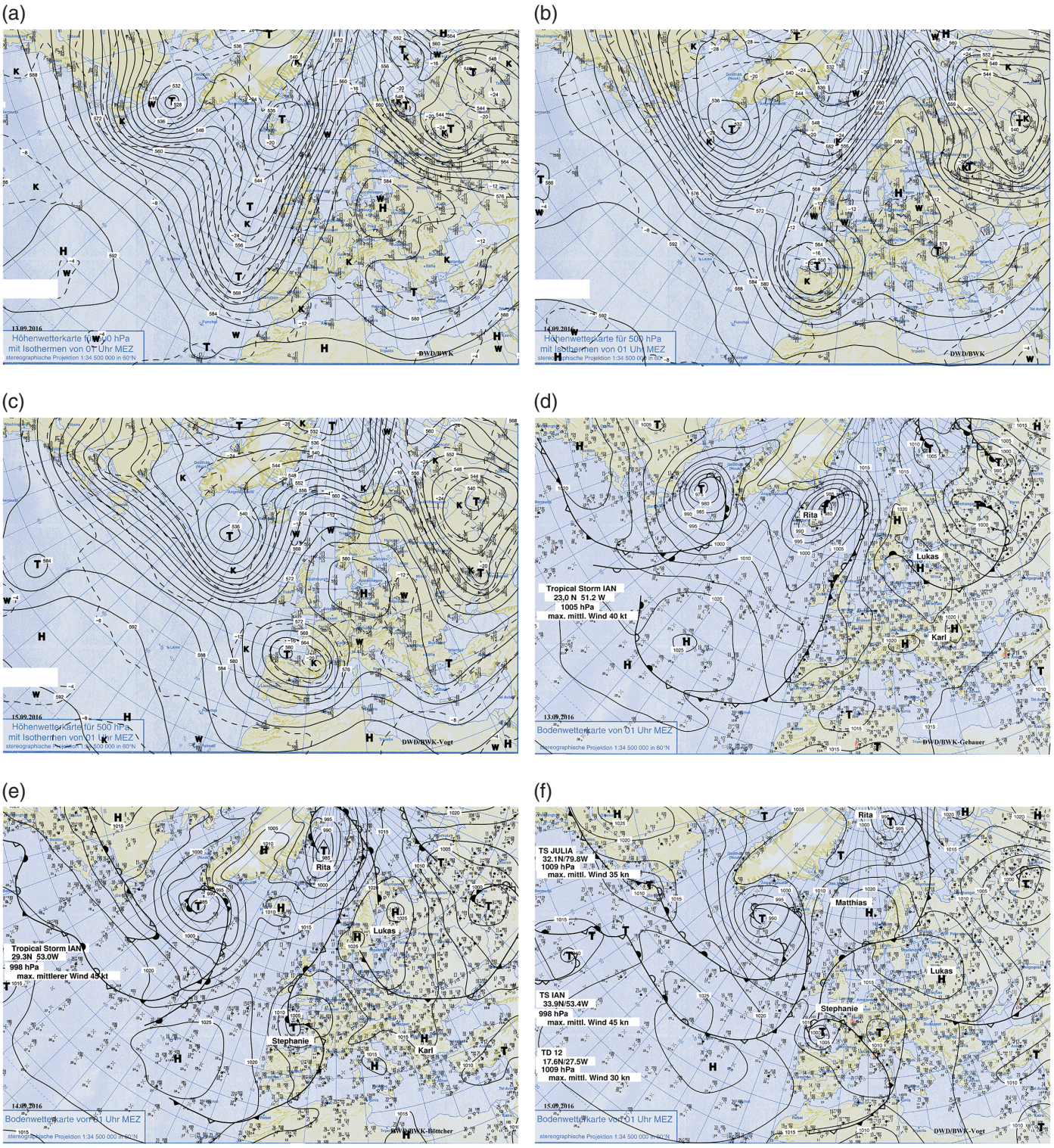

Figure 2. Synoptic charts from the Berliner Wetterkarte showing the geopotential height and the temperature at 500hPa ((a)–(c), solid and dashed contours) and the surface pressure and fronts (d–f) at 0000 UTC on 13 (a, d), 14 (b, e) and 15 (c, f) September 2016. Letters T and H mark minima and maxima in geopotential or pressure, whereas letter K and W mark minima and maxima in temperature.

Mean-sea-level pressure (MSLP) data, taken from the operational analysis of the European Centre for Medium-Range Weather Forecasts (ECMWF), allow tracking of the centre of the surface low. It was steered cyclonically around the cut-off in a loop through the entire Bay of Biscay, starting from the southeastern part (black curve in Figure 3(a)). The low deepened in the first 36h, starting from 1009hPa on 12 September at 1800 UTC, until the core pressure reached 998hPa on 14 September at 0600 UTC (black curve in Figure 3(b)). The deepening ended while the centre was located in the northern part of the loop. The system subsequently maintained the same depth until 15 September at 0600 UTC, coincident with the time of the occlusion. While it moved southeastward, the low filled until it made landfall. This gradual filling is consistent with the typical life cycle of an extratropical cyclone after achieving a barotropic structure. The increase in MSLP, however, slowed down between 1200 and 1800 UTC. It is noteworthy that this time corresponds to the appearance of the cloud-free central area in the satellite imagery (Figure 1).

The centre of the surface low is also tracked in the ECMWF deterministic fore-

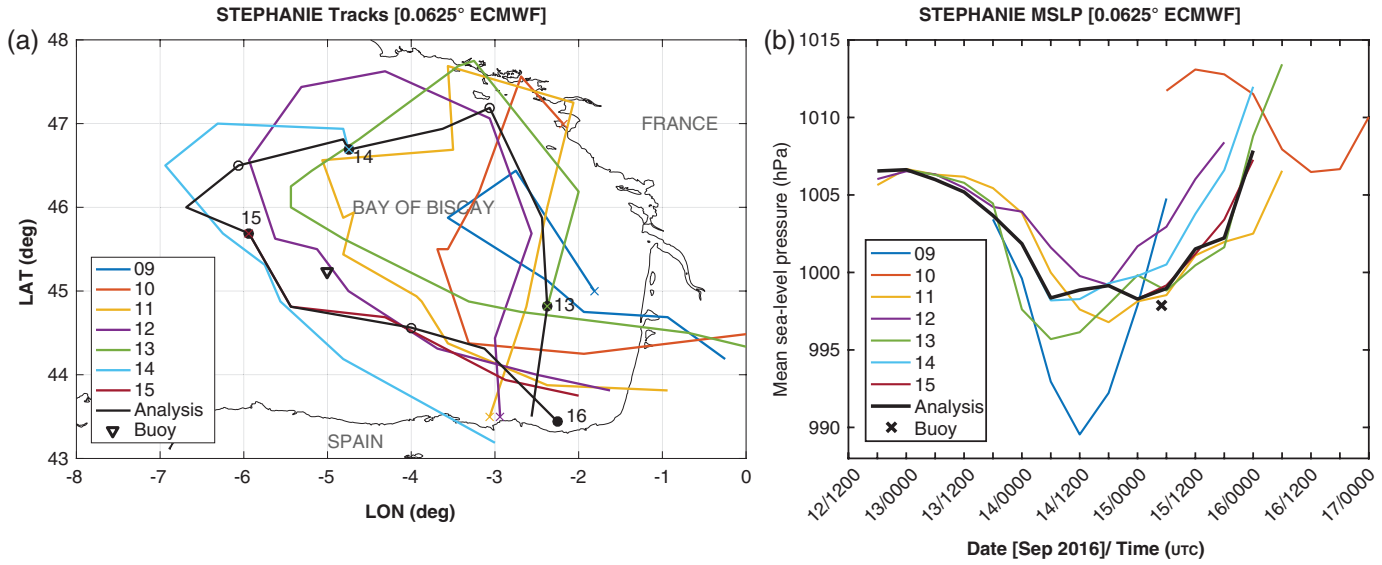

Figure 3. Track (a) and MSLP (b) of the storm in the ECMWF analysis (black curves) and deterministic forecast initialised at 0000 UTC from 9 to 15 September 2016 (coloured curves). The date is indicated for the analysis in (a), with filled and open circles representing the position at 0000 UTC and 1200 UTC, respectively. Crosses denote the starting point of each track and the triangle shows the location of the buoy Gascogne. The deepest pressure recorded by the buoy during the passage of the storm is indicated by a cross symbol in (b).

casts initialised before and during the development of the storm (coloured curves in Figure 3). The storm was first predicted in the forecast from 9 September, with previous forecasts lacking any surface low. A close look into the different forecasts indicates that for later initialisation times the storm moved farther to the west and performed a larger loop (Figure 3(a)). Landfall was predicted over France in the earlier forecasts and gradually changed towards Spain in the later forecasts. Concerning the evolution of the core pressure, the timing and minimum depth were well captured in the forecasts initialised from 11 September onwards (Figure 3(b)). In contrast, earlier forecasts predicted a storm either too deep and short-lived (9 September run) or too weak and much later (10 September run). The track and depth of the storm were thus well predicted about three days in advance.

Observations of tropical characteristics

Observations are key in understanding the structure of the storm. Fortunately, various types of in-situ and remote sensing observations cover the interesting part of the track from the end of the occlusion until landfall. Besides the MODIS satellite observation shown in Figure 1, measurements are available from a space-borne scatterometer, from a ground-based radar, from synoptic stations and from an anchored buoy.

The last 12h of the evolution, when the cyclone underwent a transition from a rather frontal to a more symmetric system, were captured by a high-resolution radar located north of Bilbao, on the Spanish coast. Figure 4 shows rain bands wrapping around the centre on 15 September at 1320 UTC, which are reminiscent of the initial stage of a tropical cyclone. This time is chosen to match the time displayed in Figure 1. In contrast to the satellite image, where the visible clouds resemble a closed ring, the radar reflectivity merely indicates a circular structure. Throughout the second half of 15 September, and until landfall, the strongest radar signal was found to the southeast of the centre. Nevertheless, the pattern allows the radius of the precipitation-free centre to be estimated at about 50km when the storm hit the Spanish coast.

Similar to tropical cyclones, Medicanes making landfall can cause devastating weather in coastal regions and on islands. In order to assess their impact, it is crucial to gather data from synoptic stations.

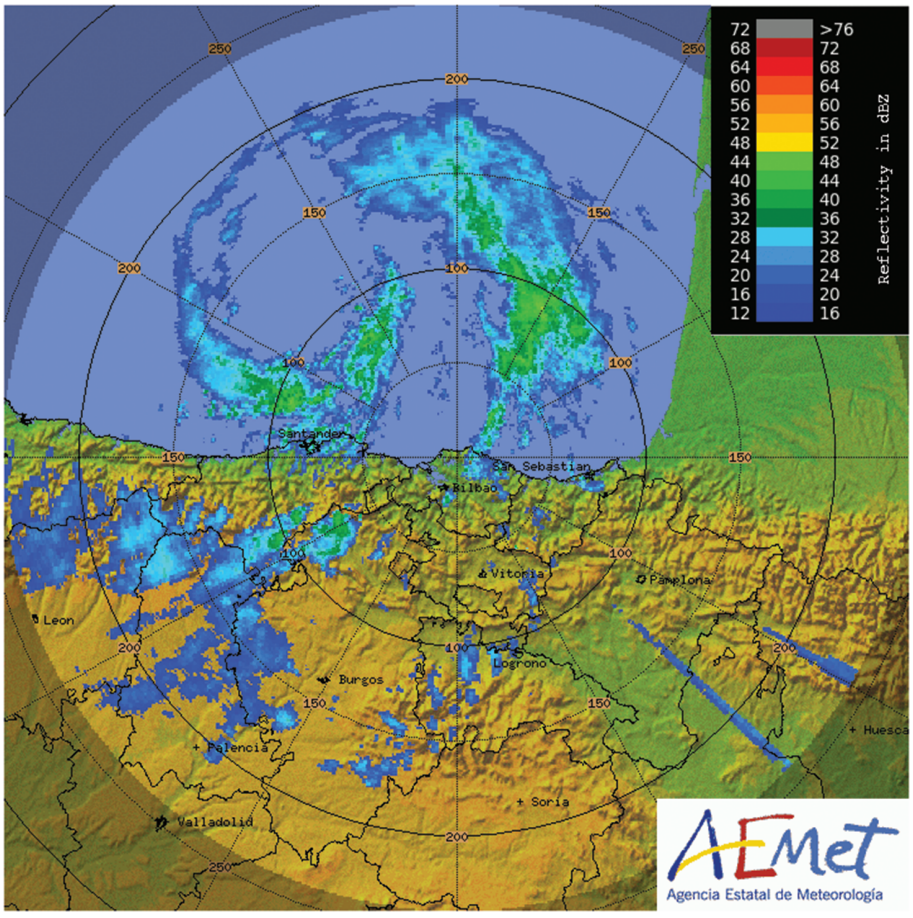

Figure 4. Radar reflectivity on 15 September 2016 at 1320 UTC. The time matches the satellite image shown in Figure 1.

Storm *Stephanie* over the Bay of Biscay was comparatively weak, but some stations recorded strong peak winds during landfall. In San Sebastian-Igueldo the maximum wind speed reached 31kn at 2100 UTC, while in Bilbao-Sondica it reached 28kn at 2200 UTC, and wind gusts of 49kn were measured at 2300 UTC. The rainfall was moderate during landfall in the Basque Country. However, heavy rain caused by the main frontal band was recorded further west. In Asturias-Aviles, 75mm were measured over a period of 12h from 0600 to 1800 UTC and resulted in flooded streets paralysing traffic. Orographic effects of the Cantabrian Mountains likely facilitated the increase in rainfall. Even though the northern Spanish region was most affected, the southwestern part of France suffered from local flooding as well. On the morning of 16 September heavy precipitation led to similar impacts in the departments Gard and Hérault near the Gulf of Lion coast.

In addition, the buoy *Gascogne* in the Bay of Biscay, which was located close to the track of the storm (and is represented by a triangle symbol in Figure 3(a)), recorded the passage of the storm centre on the morning of 15 September. Time series of pressure and wind (Figure 5) clearly indicate characteristics of a cyclonic system with a distinct, small-scale inner-core structure. Initially, the buoy measured a decreasing pressure with a minimum of 998hPa on 15 September at 0500 UTC, which is consistent with the ECMWF analysis (cross symbol on Figure 3(b)). Following this, the pressure increased at a rapid pace (Figure 5). Strong winds were recorded from late on 13 September until the morning of 15 September and reached a maximum on the afternoon of 14 September, with 38kn being recorded at 1600 UTC. This preceded a period of calm winds corresponding to the MSLP minimum, during which the wind speed dropped below 4kn. The wind speed quickly rose again 3h later to 37kn, before rapidly decreasing thereafter. Although they are not exclusive to tropical cyclones, these characteristics emphasise the symmetric and compact structure of the storm.

Wind observations derived from ASCAT scatterometers aboard the METOP satellites (Figure 6) suggest a transition from extratropical to tropical-like characteristics with respect to storm structure and intensity. A contraction and a slight intensification of the storm are seen in the wind measurements, with an evolution from a broad, asymmetric wind field with strong winds on the southwestern side on 14 September at 2040 UTC (Figure 6(a)) to a more compact and symmetric pattern with even stronger winds on 15 September at 0945 UTC (Figure 6(b)). Maximum wind speeds above 35kn on 15 September (brown barbs) are consistent with the buoy and station observations. For an actual tropical cyclone, this would correspond to tropical storm intensity on the Saffir–Simpson hurricane wind scale.

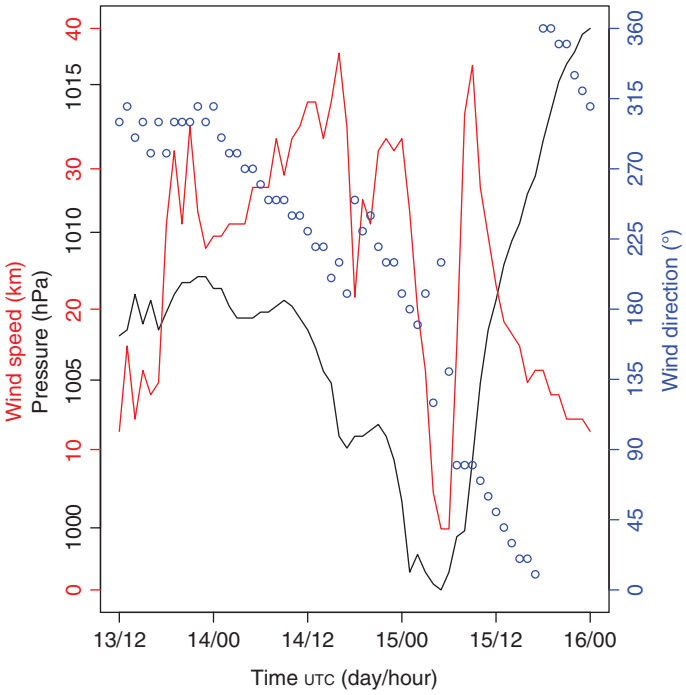

Figure 5. Pressure (black curve), wind speed (red curve) and wind direction (blue circles) recorded by the buoy Gascogne (45°13′48″N, 5°0′0″W) from 13 to 16 September 2016.

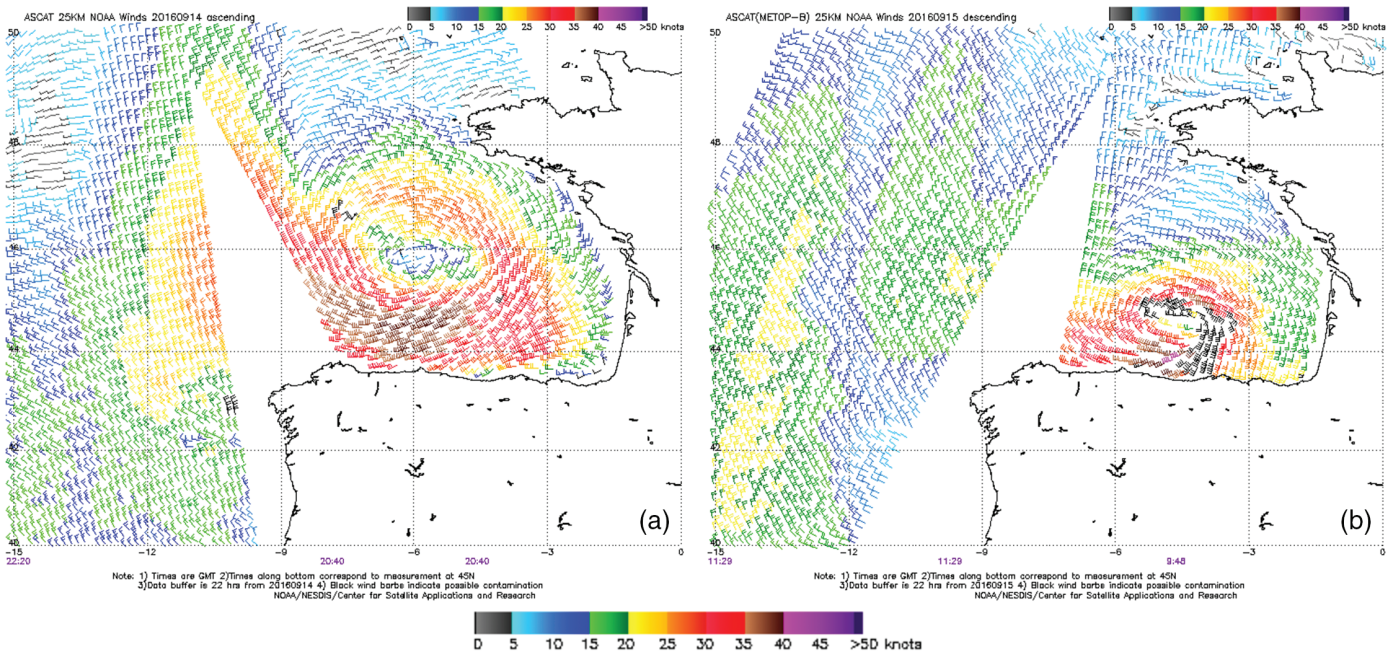

Figure 6. Wind barbs derived from ASCAT scatterometer observations on (a)14 September at 2040 UTC and (b)15 September at 0945 UTC. Black wind barbs indicate possible contamination.

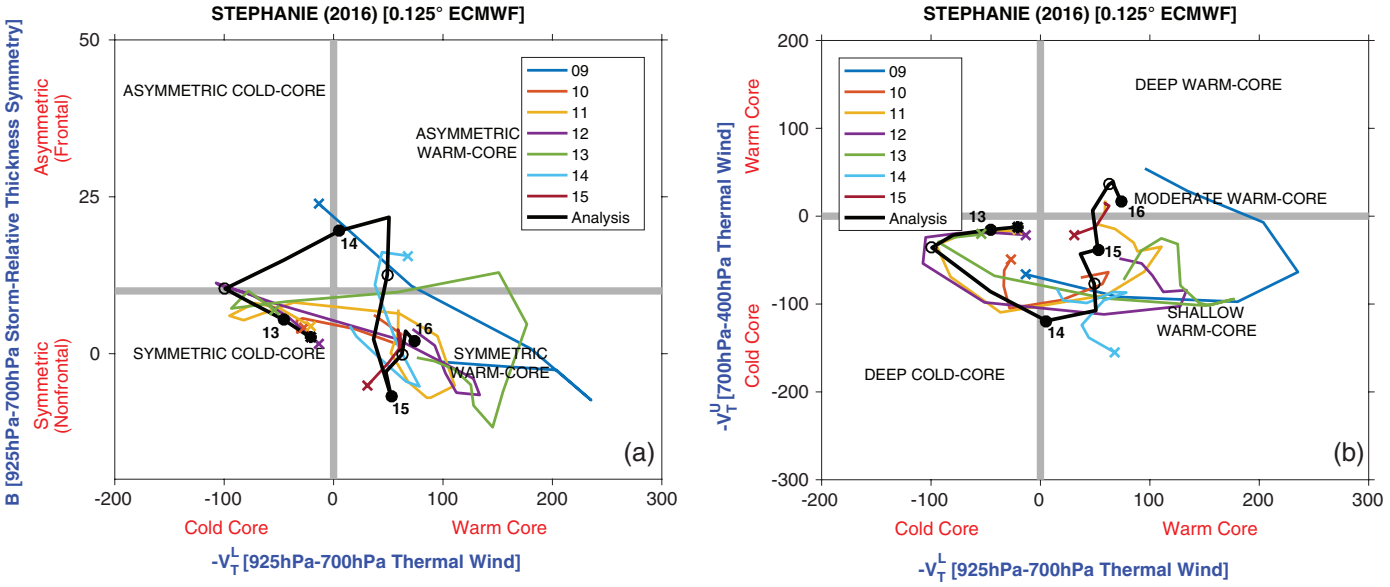

Figure 7. Cyclone phase space diagrams for the ECMWF analysis (black curves) and deterministic forecasts initialised at 0000 UTC from 9 to 15 September (coloured curves). See section titled 'Thermodynamical structure of the storm' for details. The date is indicated for the analysis, with filled and open circles representing the position at 0000 UTC and 1200 UTC, respectively. Crosses denote the starting point of each trajectory. Following Picornell et al. (2014), the original metrics of Hart (2003) are adapted to the small horizontal extent of the storm with a radius of 1.5° and to the extratropical environment with lower pressure levels. A 12h running mean is applied to all parameters to obtain smoother curves.

The set of observations described above reveals strong indications of the storm undergoing the first stages of tropical transition. A symmetrisation and contraction of the wind field surrounding the centre, sharp gradients in the wind speed on both sides of the centre during the passage of the storm and a cloud-free central area support the assumption that such a transition was taking place. This is also supported by the evolution of the thermodynamical structure described in the next section. The tropical-like phase of the storm was only short-lived, however, likely due to the fact that the storm made landfall while the transition was possibly still ongoing.

Thermodynamical structure of the storm

A powerful tool to assess changes in the thermodynamical structure of a storm during tropical transition is given by the cyclone phase space diagram developed by Hart (2003). Figure 7 shows the two components of this diagram for the evolution of the present case. Three parameters spanning a three-dimensional phase space shed light on lower-level (V^T_L) and upper-level (V^T_U) thermal wind as well as on storm-relative symmetry (B). The thermal wind is an indication of the cold or warm-core structure of the storm. A typical tropical transition is characterised by the pathway from an asymmetric cold core to a symmetric warm core (i.e. starting from the top left quadrant and running its course towards the bottom right quadrant in Figure 7(a)). However, there is a large case-to-case variability of how the transition actually happens.

The present case started its evolution as a symmetric cold-core structure, which became more and more asymmetric (black curve in Figure 7(a)). From 13 September 1200 UTC until 14 September 0600 UTC it transitioned into a warm-core system. Later, coincident with the occlusion, the storm became gradually more symmetrical. Associated with this, the warm core increased in vertical extent on 15 September (black curve in Figure 7(b)). The storm thus acquired a moderate warm-core structure before landfall.

The predictability of the tropical transition is also investigated in the ECMWF deterministic forecasts already discussed in the context of Figure 3. All forecasts predicted the symmetric warm-core structure and thus, for those initialised during the cold-core phase, the tropical transition (coloured curves in Figure 7). Most forecasts, however, underestimated or lacked the asymmetric phase and resulted in a shallow warm core. Only the earliest forecast initialised on 9 September produced a cyclone with a truly asymmetric structure that then acquired an extended warm core. The latter is consistent with this forecast predicting the deepest cyclone of all initialisations (Figure 3(b)). The tropical transition was thus captured in all forecasts that did predict the cyclone, but with different pathways.

Climatological perspective

First, we note that climatologically sea surface temperatures (SSTs) in the Bay of Biscay in autumn are particularly high for a body of water at this latitude. At the time the storm developed, SSTs exceeded 20°C over most of the area and 22°C over the southeastern part (shading in Figure 8). This is well below typical conditions over tropical waters but is comparable with Mediterranean SSTs during the development of Medicanes. In a recent study, McTaggart-Cowan *et al.* (2015) demonstrated that in an atmosphere with a cold upper troposphere and a warm boundary layer, tropical cyclogenesis can occur over SSTs considerably lower than the classical 26.5°C threshold. The authors derived a vertical coupling index based on the difference in equivalent potential temperature between the dynamical tropopause and the 850hPa pressure level. According to this index, the Bay of Biscay was in principle suitable for tropical transition during the whole lifecycle of the storm (not shown). As an additional constraint, the authors propose a new, lower threshold of 21°C in SST, which was also reached at the time the storm developed. This suggests that the environmental conditions were met for the storm to undergo tropical transition.

Compared with the long-term average for this time of year, SSTs in 2016 were warmer by 2 degC and more over a large area (contours on Figure 8). This warm anomaly was partly due to the blocking situation that prevailed over western Europe during the second week of September and which was accompanied by new maximum temperature records, as mentioned earlier. Averaged over the entire Bay of Biscay, SSTs were the highest for that time of year since the beginning of high-resolution satellite records in 1981 (Figure 9). Although the time series of SSTs exhibits a large interannual variability, a linear trend suggests a warming of more than 1 degC during the past 35 years. This value is consistent with a study of Costoya *et al.* (2015), who found a significant warming over the Bay of Biscay, particularly in autumn, accompanied by an increase in hot days. If that warming continues into the future, the Bay of Biscay may provide favourable conditions for tropi-

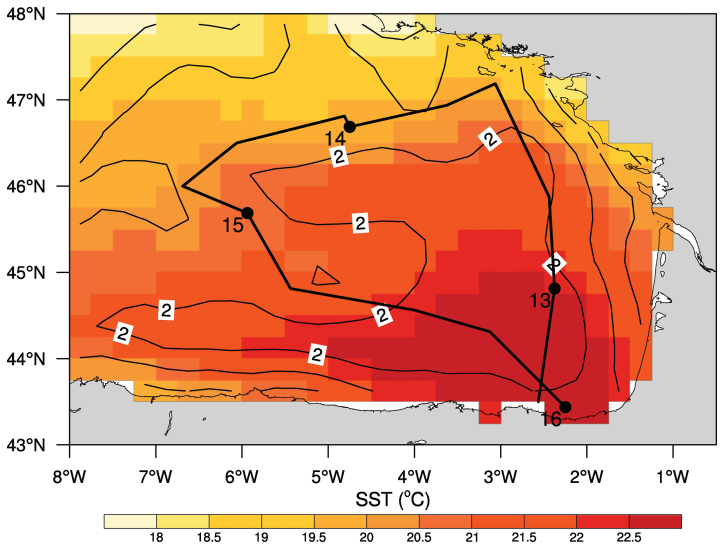

Figure 8. Average sea surface temperature during 7–13 September 2016 (shading), and anomaly with respect to the 1981–2015 average for this time of year (contours every 0.5 degC). The data are the daily Optimum Interpolation Sea Surface Temperature retrieved from the Advanced Very High Resolution Radiometer sensor using the algorithm of Reynolds et al. *(2007). The black curve shows the track of the storm in the ECMWF analysis, with dots and the date every day at 0000 UTC.*

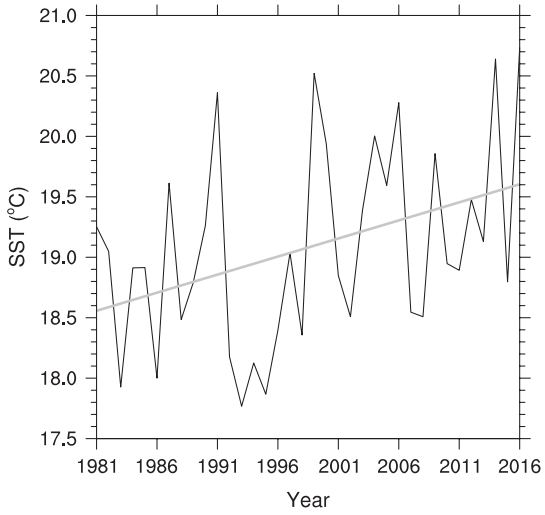

Figure 9. Average SST during the second week of September over the Bay of Biscay as shown on Figure 8 (black curve) and linear trend (grey line). See Figure 8 for details.

cal transition in autumn more frequently, and the unique tropical-like storm observed in mid-September 2016 may not be the last one of its kind. Just as Medicanes are occasionally observed over the Mediterranean Sea, Biscanes may become more familiar over the Bay of Biscay.

Conclusions

Observations and model data show that storm *Stephanie*, which cyclonically looped across the Bay of Biscay, exhibited tropical characteristics on 15 September 2016. A cloud-free central area was observed in satellite imagery and matched a ring-shaped pattern of rain in ground-based radar reflectivity. An axisymmetric wind field reaching an intensity equivalent to a tropical storm was observed from a space-borne scatterometer and confirmed by in-situ measurements from a buoy that the storm centre passed. A warm core extending to the mid troposphere and a symmetric structure were found in the ECMWF analysis. This emphasises the ongoing tropical transition of the storm, which took place during the occlusion phase and appeared to be aborted by the landfall over the Basque Country. The thermodynamical structure of the storm was well forecast at lead times up to 4 days, as were its track and intensity.

As in the case of Medicanes, the presence of a cut-off low–in this case over the Bay of Biscay is suggested to be a crucial factor for the tropical transition. Another favourable factor is identified in the unusually high SSTs. The parallels with Medicanes motivated us to name this system a Biscane. To the best of our knowledge, this is the first-ever scientific description of such a system over this region, but the strong warming trend of the waters of the Bay of Biscay suggests that Biscanes may become more frequent in the future.

Acknowledgements

We thank NASA Worldview for the MODIS satellite observations, Berliner Wetterkarte (DWD/FU Berlin) for the weather charts, DWD for access to the ECMWF analysis and forecast, AEMET for the radar observations, NOAA NCEI for the buoy and SST data and OSWT for the ASCAT observations. We also thank the editor, Jim Galvin, for his support, and an anonymous reviewer for his/her constructive comments on the manuscript. This study was funded by the DFG Collaborative Research Center 165 *Waves to Weather*, projects C3 *Multi-scale dynamics and predictability of Atlantic Subtropical Cyclones and Medicanes* and C5 *Forecast uncertainty for peak surface gusts associated with European cold-season cyclones*.

References

Billing H, Haupt I, Tonn W. 1983. Evolution of a hurricane-like cyclone in the Mediterranean Sea. *Beitr. Phys. Atmos.* **56**: 508–510.

Costoya X, de Castro M, Gómez-Gesteira M *et al.* 2015. Changes in sea surface temperature seasonality in the Bay of Biscay over the last decades (1982–2014). *J. Mar. Syst.* **150**: 91–101.

Davis CA, Bosart LF. 2004. The TT problem. *Bull. Am. Meteorol. Soc.* **85**: 1657–1662.

Emanuel K. 2005. Genesis and maintenance of "Mediterranean hurricanes". *Adv. Geosci.* **2**: 217–220.

Ernst JA, Matson M. 1983. A Mediterranean tropical storm? *Weather* **38**: 332–337.

Fita L, Romero R, Luque A *et al.* 2007. Analysis of the environments of seven Mediterranean tropical-like storms using an axisymmetric, nonhydrostatic, cloud resolving model. *Nat. Hazards Earth Syst. Sci.* **7**: 41–56.

Hart RE. 2003. A cyclone phase space derived from thermal wind and thermal asymmetry. *Mon. Weather Rev.* **131**: 585–616.

McTaggart-Cowan RE, Davies L, Fairman JG *et al.* 2015. Revisiting the 26.5°C sea surface temperature threshold for tropical cyclone development. *Bull. Am. Meteorol. Soc.* **96**: 1929–1943.

Picornell MA, Campins J, Jansà A. 2014. Detection and thermal description of medicanes from numerical simulation. *Nat. Hazards Earth Syst. Sci.* **14**: 1059–1070.

Reynolds RW, Smith TM, Liu C *et al.* 2007. Daily high-resolution-blended analyses for sea surface temperature. *J. Clim.* **20**: 5473–5496.

Correspondence to: Florian Pantillon

florian.pantillon@kit.edu

doi:10.1002/wea.2995